Construction and Building Materials 183 (2018) 163–170

Contents lists available at ScienceDirect

Construction and Building Materials

journal homepage: www.elsevier.com/locate/conbuildmat

Using Response Surface Methodology and providing a modified model using whale algorithm for estimating the compressive strength of columns confined with FRP sheets

Yaser Moodi [a], Seyed Roohollah Mousavi [a,*], Alireza Ghavidel [a], Mohammad Reza Sohrabi [a], Mohsen Rashki [b]

[a] Civil Engineering Department, University of Sistan and Baluchestan, Zahedan, Iran
[b] Department of Architecture Engineering, University of Sistan and Baluchestan, Zahedan, Iran

HIGHLIGHTS

- A modified model proposed to predict the compressive strength of FRP-confined columns.
- In the modified model, the effective strain coefficient of FRP and cross section coefficient considered as an individual coefficient.
- RSM used for efficient estimating the compressive strength of FRP-confined columns.

ARTICLE INFO

Article history:
Received 26 September 2017
Received in revised form 30 May 2018
Accepted 9 June 2018

Keywords:
Response Surface Methodology
Columns
FRP confinement
Compressive strength
Strengthening
Whale algorithm

ABSTRACT

This study presented a modified model for determining the compressive strength of square and rectangular concrete columns using whale algorithm and a widespread database. In this model, the effective strain coefficient of FRP and cross section coefficient considered as an individual coefficient. Furthermore, the coefficients of the rising strength for specimens with unconfined compressive strength in upper and lower of 35 MPa are differently considered. In addition, Response Surface Methodology used for estimating the compressive strength of the confined specimens by FRP. Finally, results compared with the existing models. The predictions of the modified model and RSM show satisfactory estimations. So that RSM and the modified model have increased R^2 approximately 34% and 26% rather other models, respectively.

1. Introduction

Most of existing reinforced concrete columns are in need of retrofitting and strengthening for various reasons, including errors during the construction phase, designing mistakes, changing the type of applications in structures, corrosion of steel and reinforcement, changes in design codes, occurrence of strong beam-weak column mechanism and the damages due to natural disasters such as earthquake, wind, flood and etc. In addition, the destruction and rebuilding of these columns are costly and often impractical. It should be noted that the strengthening and retrofitting techniques are affordable and reliable [1]. FRP is usually used for strengthening of existing reinforced concrete columns. One of the first experimental studies on FRP-confined concrete columns was presented by Nanni and Bradford in 1994 [2]. Their specimens included the wrapped concrete with ordinary strength by three kinds of FRP under uniaxial compressive loading. By investigating on stress-strain curves, they showed that compressive strength and ductility are raised by using FRP confinement. Different studies conducted for estimating compressive strength of square and rectangular columns that have been wrapped by FRP [3–8]. It is noted that most of the proposed models were presented by limit specimens in the past.

Response Surface Methodology (RSM) is one of the effective estimation methods [9]. This method is containing of several statistical and mathematical techniques to estimate a model. RSM purpose is optimization of response (output parameter) by considering input parameters. RSM proposed by Box and Wilson in 1951, firstly, then it used in different subjects [10]. RSM was modified by

* Corresponding author.
E-mail addresses: y.moodi.civil@pgs.usb.ac.ir (Y. Moodi), s.r.mousavi@eng.usb.ac.ir (S.R. Mousavi), a.r.ghavidel@pgs.usb.ac.ir (A. Ghavidel), sohrabi@hamoon.usb.ac.ir (M.R. Sohrabi), Mrashki@eng.usb.ac.ir (M. Rashki).

https://doi.org/10.1016/j.conbuildmat.2018.06.081
0950-0618/

different scholars during time [11–14]. In this study, RSM is used to estimate the compressive strength of confined specimens by FRP since RSM lead to an optimize response. Finally, the efficiency of RSM is investigated as well.

In this study, at the first step, experimental data of square and rectangular concrete specimens that confined by FRP collected from the available papers. It is noted that a wider range of statistical population lead to the more reliable results for modeling purpose. The used statistical population of this study is wider rather the previous researches. Consequently, a model is proposed to estimate the compressive strength of square and rectangular concrete columns confined by FRP based on Lam and Teng model [5]. In this study, FRP strain efficiency factor (k_ε) and section shape coefficient (k_a) are considered as single unit coefficient ($(k_\varepsilon)_{new}$), it means that hoop strain coefficient of FRP has been considered as a function of section shape. Pham and Hadi [6] assumed that the confined stress just happen at corner of section while in this study, neighborhood areas of corners are considered as well. Hence, a modified coefficient is presented as ratio of circumference of stress concentration to the total circumference of section. In addition, increasing the strength for concretes with unconfined strength lower and bigger from 35 MPa are considered differently. To this purpose, whale algorithm was used to calculate the required coefficients. As mentioned before, RSM was used to estimate the compressive strength of square and rectangular specimens that confined by FRP. The results of the proposed model and RSM model are verified using experimental data. The outputs showed that the proposed model and RSM model decrease errors in comparison with the other mentioned models. Averagely, the proposed model and RSM model in comparison with other examined models, reduced the general error about 50% and 62% for specimens that used as instructor, respectively. This reduction is approximately 38% and 36% for appraiser specimens.

2. Some existing models for the prediction of compressive strength of FRP-confined rectangular and square concrete columns

Different models have been proposed to estimate the compressive strength of square and rectangular columns confined by FRP, in the past. Some of those are summarized in Table 1 for comparison purpose.

In the study of Lam and Teng [5], effective strain factor (k_ε) is defined as ratio of the FRP actual hoop rupture strain to ultimate tension strain of FRP materials. This factor in their study was considered 0.851, 0.856, 0.624 and 0.788 for AFRP, CFRP, GFRP and HM-CFRP, respectively. Moreover, in the mentioned study, section shape factor (k_a) is related to the confined effective area and ratio of faces (b/h). In a rectangular cross-section just some zones are confined at the cross direction, effectively. They assumed the concrete that confined effectively is consist of four parabolas which cut corners with 45 degree. In Pham and Hadi [6], section shape coefficient was defined as the ratio of the total length of four rounded corners (for preventing from stress concentration) to total circumference of section. It to be account that in Pham and Hadi study, if the radius of corner be zero, the confined stress ($f_{l,a}$) would be undefined and calculation the compressive strength of confined concrete will be impractical. Section shape coefficient in the study of Harajli et al. [3], Ilki and Kumbasar [4] and Toutanji et al. [8] was considered such as Lam and Teng [5] model.

3. Experimental data

Many studies have been conducted on the confined concrete with FRP. In this study, a statistical population with 416 square and rectangular concrete specimens confined by FRP are extracted from references as follow:

Al-Salloum [15], Benzaid et al. [16], Compione [17], Compione et al. [18], Carrazedo [19], Challal et al. [20], Demers and Neale [21], Erdil et al. [22], Harajili et al. [3], Harries and Carey [23], Hosotani et al. [24], Ignatowski and Kaminska [25], Ilki and Kumbasar [4], Lam and Teng [5], Masia et al. [26], Mirmiran et al. [27], Modarelli et al. [28], Parvin and Wang [29], Rochett and Labossiere [30], Rousakis et al. [31], Rousakis and Karabinis [32], Shehata et al. [33], Suter and Pinzelli [34], Tao et al. [35], Wang and Wu [36–38], Wang et al. [39–40], Wu and Wei [41], Yan et al. [42], Yeh and Chang [43], Youssef et al. [44], Zhang et al. [45].

Exiting square and rectangular specimens of this statistical population are including the width of 70–450 mm, the length of 70–600 mm, corner radius offset of 0–60 and the unconfined compressive strength of 10–101.2 MPa. Different types of FRPs are CFRP, AFRP and GFRP. All the FRP sheets in which used in this data are one-direct (hoop direction). Monototic loading applied for the used specimens in this database. Experimental specimen details are shown in Table 2. Among these specimens, 360 specimens are used

Table 1
Some of available models for compressive strength prediction of FRP-confined rectangular and square concrete columns.

References	Model	Description
Harajli et al. [3]	$f'_{cc} = f'_c\left(1 + 1.25\sqrt{\frac{k_a \rho_f E_{frp} \varepsilon_{fe}}{2f'_c}}\right)$	$k_a = 1 - \frac{(b-2r)^2+(h-2r)^2}{3bh}$ $\rho_f = \frac{4t_j}{D},\ \ D = \frac{2bh}{b+h}$
Ilki and Kumbasar [4]	$f'_{cc} = f'_c(0.6 + 0.2\frac{b}{h})\left(1 + 2.29\left(\frac{f_{l,a}}{f'_c}\right)^{0.87}\right)$	$f_{l,a} = \frac{k_a \rho_f F_{frp}}{2},\ \ \rho_f = \frac{2t_j(b+h)}{bh}$ $k_a = 1 - \frac{(b-2r)^2+(h-2r)^2}{3bh} - \frac{(4-\pi)r^2}{bh}$
Lam and Teng [5]	$f'_{cc} = f'_{co}\left(1 + 3.3k_a\frac{f_{l,a}}{f'_{co}}\right)$	$f_{l,a} = \frac{2E_{frp}t_j\varepsilon_{h,rup}}{D}$ $\varepsilon_{h,rup} = k_\varepsilon \varepsilon_{frp}, D = \sqrt{b^2+h^2}$ $k_a = (\frac{b}{h})^2\left[1 - \frac{(\frac{b}{h})(h-2r)^2+(\frac{h}{b})(b-2r)^2}{3A_g}\right]$
Pham and Hadi [6]	$f'_{cc} = f'_{co}\pi\left(0.68 + 3.91k_a\frac{f_{l,a}}{f'_{co}}\right)$	$f_{1,a} = \frac{E_{frp}t_j\varepsilon_{h,rup}}{r}$ $k_\varepsilon = 0.5 + 0.642\ln(A)$ $A = \frac{2r}{bR_s}, R_s = \frac{t_j E_{frp}}{\left(\frac{f'_{cc}}{\varepsilon_{co}}\right)r}$ $\varepsilon_{co} = (-0.067f'_{co^2} + 29.9f'_{co} + 1053)10^{-6}$ $k_\varepsilon = \frac{\pi r}{b+h-(4-\pi)r}$
Wei and Wu [7]	$f'_{cc} = f'_c(1 + 2.2(\frac{2r}{b})^{0.72}\left(\frac{f_{l,a}}{f'_c}\right)^{0.72}(\frac{h}{b})^{-1.9}$	$f_{l,a} = \frac{2F_{frp}t_j}{b}$
Toutanji et al. [8]	$f'_{cc} = f'_c + 4(\frac{2r}{D})^{0.1}(\frac{h}{b})^{0.13}k_a f_{l,a}$	$f_{l,a} = \frac{2E_{frp}\varepsilon_{fe}t_j}{D},\ \ D = \frac{2bh}{h+b}$ $k_a = 1 - \frac{(b-2r)^2+(h-2r)^2}{3bh}$

Table 2
The collected experimental specimen details for proposing the model.

Number	References	Specimens Number	Fiber Type	B (mm)	H (mm)	r (mm)	fc(MPa)
1	Al-Salloum [15]	8	CFRP	150	150	5–50	26.7–31.8
2	Benzaid et al. [16]	6	GFRP	100	100	0–16	54.8
3	Compione [17]	2	CFRP	150	150	3	13
4	Compione et al. [18]	1	CFRP	152	152	3	20.1
5	Carrazedo [19]	4	CFRP	150	150	10–30	33.5–36.5
6	Challal et al. [20]	24	CFRP	95.25–133.35	133.35–190.5	25.4	21.4–55.4
7	Demers and Neale [21]	5	CFRP, GFRP	152	152	5	32.3–42.2
8	Erdil et al. [22]	1	CFRP	150	150	25	10
9	Harajili et al. [3]	9	CFRP	79–132	132–214	15	18.9–21.5
10	Harries and Carey [23]	4	GFRP	152	152	11–25	31.2–32.4
11	Hosotani et al. [24]	4	CFRP, HM CFRP	200	200	30	38.1
12	Ignatowski and Kaminska [25]	3	CFRP	100–105	100–200	10	32.3
13	Ilki and Kumbasar [4]	12	CFRP	150–250	250–300	40	32.8–34
14	Lam and Teng [5]	12	CFRP	150	150–225	15–25	24–41.5
15	Masia et al. [26]	15	CFRP	100–150	100–150	25	21.3–25.7
16	Mirmiran et al. [27]	9	CFRP	152.5	152.5	6.35	40.6
17	Modarelli et al. [28]	6	CFRP, GFRP	150	150–200	10–25	17.6–25
18	Parvin and Wang [29]	2	CFRP	108	108	8.26	22.6
19	Rochett and Labossiere [30]	26	CFRP, AFRP	152	152–203	5–38	35.8–43.9
20	Rousakis et al. [31]	15	CFRP, GFRP	200	200	30	33–39.9
21	Rousakis and Karabinis [32]	4	CFRP, GFRP	200	200	30	25.5
22	Shehata et al. [33]	8	CFRP	94–150	150–188	10	23.7–29.5
23	Suter and Pinzelli [34]	16	CFRP, GFRP, AFRP, HM CFRP	150	150	5–25	33.9–36.7
24	Tao et al. [35]	24	CFRP	150	150–300	20–50	19.5–49.5
25	Wang and Wu [36]	60	CFRP	150	150	0–60	29.3–55.2
26	Wang and Wu [37]	9	AFRP	100	100	10	46.4–101.2
27	Wang and Wu [38]	15	AFRP	70–150	70–150	7–15	34.6–52.1
28	Wang et al. [39]	10	CFRP	100–400	100–400	10–45	24.4
29	Wang et al. [40]	8	CFRP	204–305	204–305	20–30	25.5
30	Wu and Wei [41]	30	CFRP	150	150–300	30	32.3–42.4
31	Yan et al. [42]	2	CFRP, GFRP	279	279	19	15.2
32	Yeh and Chang [43]	28	CFRP	150–450	150–600	30	20.6
33	Youssef et al. [44]	37	CFRP, GFRP	254–381	381	38	29.2–38.7
34	Zhang et al. [45]	2	AFRP	150	150	15	45–50

for modeling (instructor specimens) and 56 specimens are selected for evaluating (appraiser specimens), randomly.

4. RSM for estimating the compressive strength of square and rectangular columns that confined by FRP

The main intention of RSM is to estimate a complex and real function with a simple and implicit function. In mathematical viewpoint, each order of a polynomial in a Taylor expansion environs the selected random points can be used to predict the appropriate response. Researchers have generally recommended the second order polynomial [46,47]. Hence, the second order of Taylor expansion is defined as follow:

$$f(X) = \beta_0 + \sum_{i=1}^{n} \beta_i X_i + \sum_{i=1}^{n} \beta_i X_i^2 + \sum_{i}^{n-1} \sum_{j=i+1}^{n} \beta_{ij} X_i X_j \quad (1)$$

In which f(x) is the desire response, X is random variables and β is unknown coefficients. To determine the unknown coefficients, function may transform to the linear regression model. In other word, the second order terms will changed to the one-order terms as follow:

$$y = \beta_0 + \beta_1 X_1 + \beta_2 X_2 + \ldots + \beta_k X_k + \varepsilon \quad (2)$$

in which ε is the error. The above equation can rewrite as:

$$y = \beta X + \varepsilon \quad (3)$$

The matrix coefficient is calculated using least squares approach as follow:

$$\beta = (XX)^T X^T y \quad (4)$$

In this study, the compressive strength is estimated by considering of combined terms. To this aim, seven parameters are considered as input variables including b, h, r, f_{co}, t_f, F_f, E_f and output is considered as f_{cc}. A second-order polynomial was fitted to the output of experimental data based on input variables. The coefficients of this polynomial were calculated by subject to error minimum between the experimental and estimated data. This response function has $R^2 = 0.79$ and 11.11% error for learner data and for data that never used to estimate of response function are $R^2 = 0.83$ and 11.64% error.

5. The proposed model to predict the compressive strength of confined square and rectangular columns with FRP

Square and rectangular concrete columns confined by FRP are failed suddenly due to rupturing of FRP. In these specimens, the ruptured conditions are happened in the corner areas of section [30,40,48,49]. Hence, when specimens are failed, the hoop strain of FRP is the highest value at the corner area. In this study is shown that the effective strain factor is correlated to the section shape in the square and rectangular sections which this factor may calculated by averaging of strains at the section circumference and consequently it can be used to estimate the average FRP hoop stress. To this aim, suppose that strain at corners and their neighborhoods regions of the section is equal to ultimate strain of FRP and at the others areas, strain is low. Hence, the confined stress at corners and those neighborhood regions of the section is maximum and at the others areas is zero. As shown in Fig. 1, there are some segments with αb and βh dimensions where FRP strain reaches to the ultimate strain. As it is described above, the FRP strain efficiency factor is determined as a function of section shape as follow:

$$(k_\varepsilon)_{new} = k_\varepsilon k_a = \frac{\pi r + \alpha b + \beta h}{b + h - (4 - \pi) r} \quad (5)$$

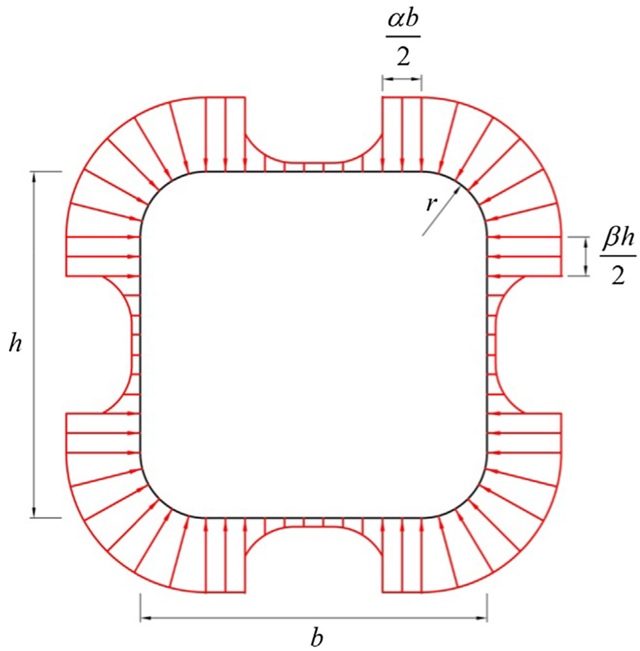

Fig. 1. Modified distribution of confining stress.

In this study, the increased value of strength is considered differently for the specimens with the compressive strength less or more than 35 MPa. It means that the increased value considered as follow:

$$\begin{cases} f'_{cc} = f'_{co}\left(1 + \gamma(k_\varepsilon)_{new}\frac{f_{l,a}}{f'_{co}}\right) & f'_{co} \leqslant 35MPa \\ f'_{cc} = f'_{co}\left(1 + \lambda(k_\varepsilon)_{new}\frac{f_{l,a}}{f'_{co}}\right) & f'_{co} > 35MPa \end{cases} \tag{6}$$

The unconfined compressive strength of 35 MPa was selected based on average of specimen strengths shown in Table 2. The coefficient of α, β, γ and λ may be calculated by optimizing using whale optimization algorithm (WOA). To this aim, the total error (e_{tot}) makes minimum using Eq. (7):

$$e_{tot} = 100 * \frac{\sum_1^N |Expe_i - Theo_i|}{\sum_1^N |Expe_i|} \tag{7}$$

In which $Expe_i$ and $Theo_i$ are the experimental compressive strength (from experimental data were presented in section experimental data) and the compressive strength results of theoretical model, respectively. N is the total samples. The proposed model is the same as that used by Lam and Teng model [5] while the proposed model used one coefficient based on Eq. (5) instead of using coefficient of section shape and effective strain coefficient of FRP. In addition, in the proposed model the increased strength value is considered different between specimens with the compressive strength of less 35 or more than 35 MPa.

6. Whale optimization algorithm (WOA)

Whale Optimization Algorithm is an algorithm that copy catting from the nature. Meta-heuristic algorithms are popular in engineering applications due to: 1. Learning and running of these algorithms are roughly simple, 2. Gradient information in not required, 3. Able to leave the local optimal points, 4. They are used in widely range of scientific fields [50].

Whale algorithm is based on hunting of humpback whales. Foraging behavior of these whales is named the finding bubble-net. Its mathematical model and optimization algorithm are summarized as follows [50]:

6.1. Encircling of prey

humpback whales recognize the location of prey and encircle them. The WOA algorithm assumes that the current best candidate solution is the target prey or is close to the optimum. After the best search agent is defined, the other search agents will hence try to update their positions towards the best search agent. This behavior is represented by the following equations:

$$\vec{D} = \left|\vec{C}.\vec{X}^*(t) - \vec{X}(t)\right| \tag{8}$$

$$\vec{X}(t+1) = \vec{X}^*(t) - \vec{A}.\vec{D} \tag{9}$$

$\vec{A}$ and $\vec{C}$ are the coefficient vectors:

$$\vec{C} = 2.\vec{r} \tag{10}$$

$$\vec{A} = 2\vec{a}.\vec{r} - \vec{a} \tag{11}$$

where t indicates the current iteration, $\vec{X}^*$ is the best position vector obtained so far, $\vec{X}$ indicates the position vector of a whale. $\vec{a}$ is linearly decreased from 2 to 0 over the course of iterations, $\vec{r}$ random vectors in [0,1] and is a multiplying of element in other element. Eq. (9) allows the each search agent to update their position into the best position and simulate the encircling.

6.2. Bubble-net attacking method

Two process were presented for this method:

a) Shrinking encircling mechanism: This behavior is achieved by decreasing the value of $\vec{a}.\vec{A}$ is a random variable in the interval [−a, a]. Setting random values for $\vec{A}$ in [−1,1], the new position of a search agent can be defined anywhere in between the original position of the agent (x,y) and the position of the current best agent (x*,y*).
b) Spiral updating position: This approach first calculates the distance between the whale located at (X,Y) and prey located at (X*,Y*). A spiral equation is then created between the position of whale and prey:

$$\vec{X}(t+1) = \vec{D}'.e^{bl}.cos(2\pi l) + \vec{X}^*(t) \tag{12}$$

$$\vec{D}' = \left|\vec{X}^*(t) - \vec{X}(t)\right| \tag{13}$$

where $\vec{D}'$ indicates the distance of the i-th whale to the prey, b is a constant for defining the shape of the logarithmic spiral, and t is a random number in [−1,1].

Humpback whales swim around the prey within a shrinking circle and along a spiral-shaped path simultaneously. To simulate this behavior, it is assumed that there is a probability of 50% to choose between two mechanisms:

$$\vec{X}(t+1) = \begin{cases} \vec{X}^*(t) - \vec{A}.\vec{D} & p < 0.5 \\ \vec{D}'.e^{bl}.cos(2\pi l) + \vec{X}^*(t) & p \geqslant 0.5 \end{cases} \tag{14}$$

6.3. Search for prey

Based on the variation of the $\vec{A}$ vector can be utilized to search for prey. If $\left|\vec{A}\right| > 1$, search agent is forced to move far away from original whale. This mechanism allows the WOA to perform a global search.

$$\vec{D} = \left|\vec{C}.\vec{X}_{rand}(t) - \vec{X}(t)\right| \quad (15)$$

$$\vec{X}(t+1) = \vec{X}_{rand}(t) - \vec{A}.\vec{D} \quad (16)$$

In which $\vec{X}_{rand}$ is a random position vector that is selected from the current population.

By optimizing on 360 experimental specimens that are randomly selected from Table 2, using search agent of 100 after 500 iteration and considering interval [0,1] for α and β, [1,5] for γ and λ, are resulted: $\alpha = 0.0524$, $\beta = 0.01$, $\gamma = 4.4852$, $\lambda = 2.4780$. It is noticed that e_{tot} in Eq. (7) is 11.67 percent for the proposed model.

Schematic code of the WOA algorithm is presented below [50]:

```
Initialize the whales population Xi(i= 1, 2, ..., n)
Calculate the fitness of each search agent
X*=the best search agent
while(t < maximum number of iterations)
  for each search agent
  Update a, A, C, l, and p
    if1(p<0.5)
      if2(|A|< 1)
        Update the position of the current search agent by the Eq.(9)
      else if2(|A|≥1)
        Select a random search agent (Xrand)
        Update the position of the current search agent by the Eq.(16)
      end if2
    else if1 (p≥0.5)
   Update the position of the current search by the Eq. (12)
    end if1
  end for
  Check if any search agent goes beyond the search space and amend it
  Calculate the fitness of each search agent
  Update X* if there is a better solution
  t=t+1
end while
return X*
```

7. Discussion and evaluating the proposed models

According to values obtained for α and β and comparing k_ε of the proposed model with k_a of Pham and Hadi model [6], it is showed that stress concentration in FRP exist in corner areas and their neighborhood, hence confined stress concentration is considered in the proposed model to improve Pham and Hadi model [6]. Moreover, the values of γ and λ show that increasing the compressive strength are various for column that have different unconfined compressive strength. The increased value is less for the higher strength. It means that the effect of FRP is less for concrete with the bigger unconfined strength. An increasing value for specimens with the strength less than 35 MPa is 1.81 times of specimens with the strength more than 35 MPa.

The proposed model in this study to predict the compressive strength of confined square and rectangular columns with FRP is summarized as bellow:

$$\begin{cases} f'_{cc} = f'_{co}\left(1 + 4.485(k_\varepsilon)_{new}\frac{f_{l,a}}{f'_{co}}\right) & f'_{co} \leqslant 35MPa \\ f'_{cc} = f'_{co}\left(1 + 2.478(k_\varepsilon)_{new}\frac{f_{l,a}}{f'_{co}}\right) & f'_{co} > 35MPa \end{cases} \quad (17)$$

$$f_{l,a} = \frac{2E_{frp}t_j\varepsilon_{frp}}{D} \quad (18)$$

$$(k_\varepsilon)_{new} = \frac{\pi r + 0.0524b + 0.01h}{b + h - (4-\pi)r} \quad (19)$$

where $(k_\varepsilon)_{new}$ is the effective strain factor of FRP that was considered as a function of section shape.

A collection of experimental data that have no effect on the modeling procedure were used for the investigation and comparison of different models. These data are the rest specimens of Table 2 (56 specimens).

To easy comprehension of performances of the proposed model and RSM in comparison with the existing models, statistical parameters are introduced. These parameters are mean square error, average absolute magnitude error, standard deviation that are given by Eqs. (20) to (22):

$$MSE = \frac{\sum_1^N \left(\frac{Theo_i - Expe_i}{Expe_i}\right)^2}{N} \quad (20)$$

$$AAE = \frac{\sum_1^N \left|\frac{Theo_i - Expe_i}{Expe_i}\right|}{N} \quad (21)$$

$$SD = \sqrt{\frac{\sum_1^N \left(\frac{Theo_i}{Expe_i} - \frac{Theo_{avg}}{Expe_{avg}}\right)^2}{N-1}} \quad (22)$$

The statistical parameters to evaluate the accuracy of the proposed model and RSM are shown in Table 3 for all specimens of Table 1. Pham and Hadi [6] model is impractical for specimens that their corner radius is zero. Hence, statistical parameters have been calculated for 386 specimens for this model.

As shown in Table 3, the proposed model and RSM are more accurate rather other models. It is noted that the proposed model

Table 3
Statistical parameters for confined concrete specimens with FRP.

Specimens	Theoretical models	etot	MSE	AAE	SD
specimen used for modeling	Harajli et al. [3]	22.67	8.00	23.26	0.22
	Ilki and Kumbasar [4]	17.50	6.60	17.36	0.26
	Lam and Teng [5]	15.84	5.26	15.56	0.23
	Pham and Hadi [6]	21.87	10.39	21.96	0.32
	Wei and Wu [7]	13.56	3.09	13.32	0.17
	Toutanji et al. [8]	16.54	5.33	16.35	0.22
	Proposed model	12.04	2.18	11.24	0.14
	RSM	11.11	2.00	11.16	0.14
specimen used for evaluation	Harajli et al. [3]	24.48	9.47	26.20	0.23
	Ilki and Kumbasar [4]	13.50	3.03	13.66	0.18
	Lam and Teng [5]	14.46	3.57	15.00	0.19
	Pham and Hadi [6]	15.76	4.35	16.16	0.21
	Wei and Wu [7]	12.57	2.68	13.20	0.16
	Toutanji et al. [8]	14.5	3.76	15.48	0.18
	Proposed model	11.50	2.18	10.75	0.13
	RSM	11.64	2.20	11.86	0.15

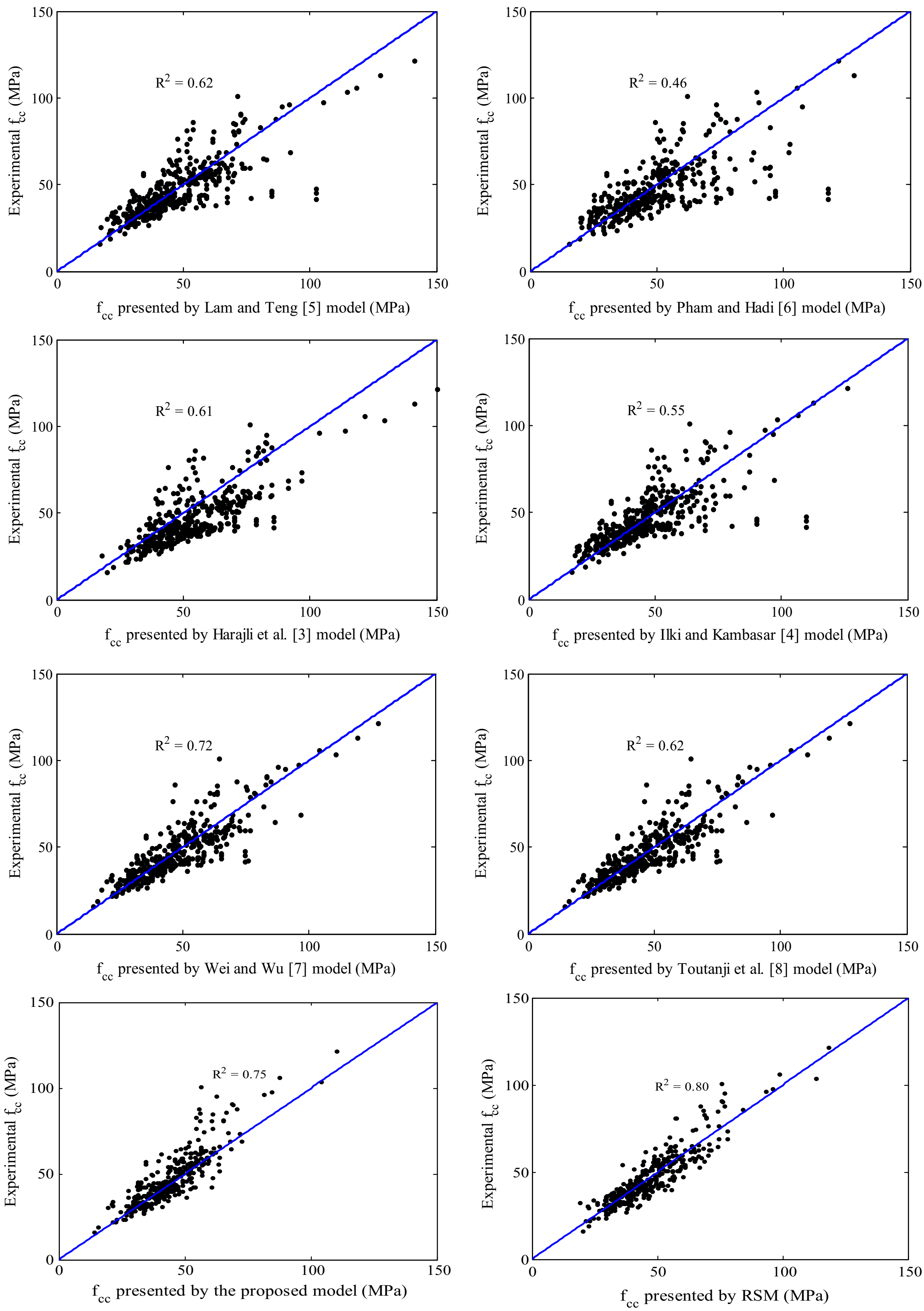

Fig. 2. Performance of models.

is caused a reduction in total error about 31%, 75%, 92%, 41%, 12% and 36% in comparisons with models of Lam and Teng [5], Pham and Hadi [6], Harajli et al. [3], Ilki and Kumbasar [4], Wei and Wu [7] and Toutanji et al. [8], respectively for the entire data (416 specimens in Table 2). Moreover, RSM lead to a reduction in total error about 40%, 87%, 105%, 51%, 20% and 45% in comparisons with models of Lam and Teng [5], Pham and Hadi [6], Harajli et al. [3], Ilki and Kumbasar [4], Wei and Wu [7] and Toutanji et al. [8], respectively for the entire data (416 specimens in Table 2). To illustrate the efficiency of the proposed model and RSM, experimental compressive strength against compressive strength resulted from the proposed model and RSM are shown in Fig. 2. This figure shows that the proposed model and RSM are in good agreement with experimental data. Correlation coefficients (R^2) are also illustrated for them. As it is seen, the best correlation coefficient is related to RSM. In other hand, R^2 for the RSM model increased about 29%, 74%, 31%, 45%, 11%, 29% and 7% in comparison with Lam and Teng [5], Pham and Hadi [6], Harajli et al. [3], Ilki and Kumbasar [4], Wei and Wu [7], Toutanji et al. [8] and the modified model, respectively. In addition, R^2 for the modified model increased about 21%, 63%, 22%, 36%, 1% and 21% in comparison with Lam and Teng [5], Pham and Hadi [6], Harajli et al. [3], Ilki and Kumbasar [4], Wei and Wu [7], Toutanji et al. [8], respectively.

8. Conclusion

In this paper, a model proposed to estimate the compressive strength of confined square and rectangular concrete columns with FRP. In addition, RSM used to predict the compressive strength of the confined square and rectangular concrete columns with FRP. In the proposed model for failure mechanism of the confined square and rectangular columns with FRP, real rupture strain of FRP happened at the corners and close to the corners. To this aim, effective strain factor is calculated as a function of section shape by averaging rupture strain of FRP at the entire of section circumference. Hereby, the results are summarized as follow:

1- The results show that in addition to the corners, there is a stress concentration near the corners that the proposed model considered this stress near of the corners by applying coefficients in cross-sectional dimensions.
2- The results show that increasing the compressive strength for columns with higher unconfined compressive strength is less. In this way, for specimens with the unconfined compressive strength less than 35 MPa is 1.81 times of specimens with the unconfined compressive strength more than 35 MPa.
3- The proposed model and RSM predict the compressive strength of the confined concrete columns with FRP, accurately. The proposed model and RSM lead to reduction of entire error about 50% and 62% for the samples used for the modeling phase, respectively. This reduction for the samples used for the evaluating phase is approximately 38% and 36% for the proposed model and RSM, respectively. Totally, statistical parameters show that RSM predict the compressive strength with more accurate rather other models.
4- RSM and the modified model are performed accurately rather other models, so that R^2 is increased about 34% and 26%, respectively.

9. Conflict of interest

The authors declare no conflict of interest.

References

[1] S.H. Ahmad, A.R. Khaloo, A. Irshaid, Behavior of concrete spirally confined by fiberglass filaments, Mag. Concr. Res. 43 (156) (1991) 143–148.
[2] A. Nanni, N.M. Bradford, FRP jacketed concrete uniaxial compression, Constr. Build. Mater. 9 (2) (1995) 115–124.
[3] M.H. Harajli, E. Hantouche, K. Soudki, Stress-strain model for fiber-reinforced polymer jacketed concrete columns, ACI Struct. J. 103 (5) (2006) 672–682.
[4] A. Ilki, N. Kumbasar, Compressive behaviour of carbon fibre composite jacketed concrete with circular and non-circular cross-sections, J. Earthquake Eng. 7 (3) (2003) 381–406.
[5] L. Lam, J.G. Teng, Design-oriented stress-strain model for FRP-confined concrete in rectangular columns, J. Reinf. Plast. Compos. 22 (13) (2003) 1149–1186.
[6] T.M. Pham, M.N.S. Hadi, Stress prediction model for FRP confined rectangular concrete columns with rounded corners, J. Compos. Constr. ASCE 18 (2014) 1–10.
[7] Y.Y. Wei, Y.F. Wu, Unified stress–strain model of concrete for FRP-confined columns, Constr. Build. Mater. 26 (2012) 381–392.
[8] H. Toutanji, M. Han, J. Gilbert, Behavior of large-scale rectangular columns confined with FRP composites, J. Compos. Constr. ASCE 14 (2010) 62–71.
[9] R.H. Myers, D.C. Montgomery, Response Surface Methodology: Process and Product Optimization Using Designed Experiments, 2nd ed., John Wiley & Sons, New York, NY, USA, 2002.
[10] G.E.P. Box, The exploration and exploitation of response surfaces: some general considerations and examples, Biometrics 10 (1954) 16–60.
[11] F.A. Wong, Slope reliability and response surface method, J. Geotech. Eng. 111 (1) (1985) 32–53.
[12] L. Faraveli, Response surface approach for reliability analysis, J. Eng. Mech. ASCE 115 (2) (1989) 2763–2781.
[13] C.G. Bucher, U. Bourgund, A fast and efficient response surface approach for structural reliability problems, Struct. Saf. 7 (1) (1990) 57–66.
[14] S.H. Kim, S.W. Na, Response surface method using vector projected sampling points, Struct. Saf. 19 (1) (1997) 3–19.
[15] Y.A. Al-Sallouni, Influence of edge sharpness on the strength of square concrete columns confined with FRP composite laminates, Compos. Part B-Eng. 38 (5–6) (2007) 640–650.
[16] R. Benzaid, N.E. Chikh, H. Mesbah, Behaviour of square concrete column confined with GFRP composite wrap, J. Civil Eng. Manage. 14 (2) (2008) 115–120.
[17] G. Campione, Influence of FRP v.-rapping techniques on the compressive behavior of concrete prisms, Cem. Concr. Compos. 28 (5) (2006) 497–505.
[18] C.L. Campione, N. Miraglia, N. Scibiha, Compressive behaviour of RC members strengthened with carbon fibre reinforced plastic layers, Adv. Earthquake Eng. 9 (2001) 397–406.
[19] R. Carrazedo, Mechanisms of confinement and its implication in strengthening of concrete columns with FRP jacketing PhD dissertation, University of Sao Paulo, 2002.
[20] O. Chaallai, M. Shahawy, M. Hassan, Performance of axially loaded short rectangular columns strengthened with carbon fiber-reinforced polymer wrapping, J. Compos. Constr. 7 (3) (2003) 200–208.
[21] M. Demers, K.W. Neale, Strengthening of concrete columns with unidirectional composite sheets, in: Proceedings of Developments in Short and medium Span Bridge Engineering, Montreal, Que, 1994.
[22] B. Erdil, U. Altyuz, I.O. Yaman, Mechanical behavior of CFRP confined low strength concretes subjected to simultaneous heating-cooling cycles and sustained loading, Mater. Struct. 45 (1–2) (2012) 223–233.
[23] K.A. Harries, S.A. Carey, Shape and "gap" effects on the behavior of variably confined concrete, Cem. Concr. Res. 33 (6) (2003) 881–890.
[24] K. Hosotani, K. Kawashima, J. Hoshikutna, A model for confinement effect for concrete cylinders confined by carbon fiber sheets, in: NCEER-INCEDE Workshop on Earthquake Engineering Frontiers of Transportation Facilities, State University of New York, Buffalo, New York, 1997.
[25] P. Ignatowski, M.E. Kamifiska, On behaviour of compressed concrete confined with CFRP composites, Eng. Build. 4 (2003) 204–208.
[26] M.J. Masia, T.N. Gale, N.G. Shrive, Size effects in axially loaded square-section concrete prisms strengthened using carbon fibre reinforced polymer wrapping, Can. J. Civ. Eng. 31 (1) (2004) 1–13.
[27] A. Mirmiran, M. Shahawy, M. Samaan, H. El Echary, J.C. Mastrapa, O. Pico, Effect of column parameters on FRP-confined concrete, J. Compos. Constr. 2 (4) (1998) 175–185.
[28] R. Modarelli, F. Micelli, O. Manni, FRP-confinement of hollow concrete cylinders and prisms, in: Proceedings of the 7th International Symposium on Fiber Reinforced Polymer Reinforcement of Reinforced Concrete Structures, 2005, pp. 1029–1046.
[29] A. Parvin, W. Wang, Behavior of FRP jacketed concrete columns under eccentric loading, J. Compos. Constr. 5 (3) (2001) 146–152.
[30] P. Rochette, P. Labossiere, Axial testing of rectangular column models confined with composites, J. Compos. Constr. 4 (3) (2000) 129–136.
[31] T.C. Rousakis, A.I. Karabinis, P.D. Kiousis, FRP-confined concrete members: Axial compression experiments and plasticity modeling, Eng. Struct. 29 (7) (2007) 1343–1353.
[32] T.C. Rousakis, A.I. Karabinis, Adequately FRP confined reinforced concrete columns under axial compressive monotonic or cyclic loading, Mater. Struct. 45 (7) (2012) 957–975.

[33] I. Shehata, L.A. Cameiro, L.C.D. Shehata, Strength of short concrete columns confined with CFRP sheds, Mater. Struct. 35 (245) (2002) 50–58.
[34] R. Suter, R. Pinzelli, Confinement of concrete columns with FRP sheets, in: Proceedings of the 5th Symposuim on Fibre Reinforced Plastic Reinforcement for Concrete Structures, London, 2001, pp. 791–802.
[35] Z. Tao, Q. Yu, Y.Z. Zhong, Compressive behaviour of CFRP-confined rectangular concrete columns, Mag. Concr. Res. 60 (10) (2008) 735–745.
[36] L.M. Wang, Y.F. Wu, Effect of corner radius on the performance of CFRP-confined square concrete columns: Test, Eng. Struct. 30 (2) (2008) 493–505.
[37] Y.F. Wang, H.L. Wu, Experimental investigation on square high-strength concrete short columns confined with AFRP sheets, J. Compos. Constr. 14 (3) (2010) 346–351.
[38] Y.F. Wang, H.L. Wu, Size effect of concrete short columns confined with aramid FRP jackets, J. Compos. Constr. 15 (4) (2011) 535–544.
[39] Z. Wang, D. Wang, S.T. Smith, Size effect of square concrete columns confined with CFRP wraps, in: Proceedings of the Third Asia-Pacific Conference on FRP in Structures, Hokkaido University, Japan, SI A01, 2012.
[40] Z.Y. Wang, D.Y. Wang, S.T. Smith, D.G. Lu, CFRP-confined square RC columns. 1: experimental investigation, J. Compos. Constr. 16 (2) (2012) 150–160.
[41] Y.F. Wu, Y.Y. Wei, Effect of cross-sectional aspect ratio on the strength of CFRP-confined rectangular concrete columns, Eng. Struct. 32 (1) (2010) 32–45.
[42] Z.H. Yan, C.P. Pantelides, L.D. Reaveley, Fiber-reinforced polymer jacketed and shape-modified compression members: I – experimental behavior, ACI Struct. J. 103 (6) (2006) 885–893.
[43] F.Y. Yeh, K.C. Chang, Size and shape effects on strength and ultimate strain in FRP confined rectangular concrete columns, J. Mech. 28 (4) (2012) 677–690.
[44] M.N. Youssef, M.Q. Feng, A.S. Mosallam, Stress-strain model for concrete confined by FRP composites, Compos. Part B-Eng. 38 (5–6) (2007) 614–628.
[45] D.J. Zhang, Y.F. Wang, Y.S. Ma, Compressive behaviour of FRP-confined square concrete columns after creep, Eng. Struct. 32 (8) (2010) 1957–1963.
[46] T.W. Simpson, T.M. Mauery, J.J. Korte, F. Mistree, Comparison of response surface and Kriging models for multidisciplinary design optimization, in: 7th AIAA/USAF/NASA/ISSMO Symposium on Multidisciplinary Analysis & Optimization, St. Louis, MO, AIAA 1, 1998, pp. 381–391. AIAA-98-4755.
[47] A. Ghavidel, S.R. Mousavi, M. Rashki, The effect of FEM mesh density on the failure probability analysis of structures, KSCE J. Civ. Eng. (2017), https://doi.org/10.1007/s12205-017-1437-5.
[48] O. Chaallal, M. Shahawy, M. Hassan, Performance of axially loaded short rectangular columns strengthened with carbon fiber-reinforced polymer wrapping, J. Compos. Constr. ASCE 7 (2003) 200–208.
[49] M.N.S. Hadi, T.M. Pham, X. Lei, New method of strengthening reinforced concrete square columns by circularizing and wrapping with fiber-reinforced polymer or steel straps, J. Compos. Constr. ASCE 17 (2013) 229–238.
[50] S. Mirjalili, A. Lewis, The whale optimization algorithm, Adv. Eng. Softw. 95 (2016) 51–67.